X-ray emission current scaling experiments for compact single-tungsten-wire arrays at 80-nanosecond implosion times

Michael G. Mazarakis, Michael E. Cuneo, William A. Stygar, Henry C. Harjes, Daniel B. Sinars, Brent M. Jones, Christopher Deeney,* Eduardo M. Waisman, Thomas J. Nash, Kenneth W. Struve, and Dillon H. McDaniel
[1]*Sandia National Laboratories, Albuquerque, New Mexico 87185-1194, USA*

(Received 5 November 2007; revised manuscript received 9 July 2008; published 29 January 2009)

We report the results of a series of current scaling experiments with the *Z* accelerator for the compact, single, 20-mm diameter, 10-mm long, tungsten-wire arrays employed for the double-ended hohlraum ICF concept [M. E. Cuneo *et al.*, Plasma Phys. Controlled Fusion **48**, R1 (2006)]. We measured the *z*-pinch peak radiated x-ray power and total radiated x-ray energy as a function of the peak current, at a constant implosion time $\tau_{\mathrm{imp}}=80$ ns. Previous x-ray emission current scaling for these compact arrays was obtained at $\tau_{\mathrm{imp}}=95$ ns in the work of Stygar *et al.* [Phys. Rev. E **69**, 046403 (2004)]. In the present study we utilized lighter single-tungsten-wire arrays. For all the measurements, the load hardware dimensions, materials, and array wire number ($N=300$) were kept constant and were the same as the previous study. We also kept the normalized load current spatial and temporal profiles the same for all experiments reported in this work. Two different currents, 11.2 ± 0.2 MA and 17.0 ± 0.3 MA, were driven through the wire arrays. The average peak x-ray power for these compact wire arrays increased by $26\%\pm7\%$ to 158 ± 26 TW at 17 ± 0.3 MA from the 125 ± 24 TW obtained at a peak current of 18.8 ± 0.5 MA with $\tau_{\mathrm{imp}}=95$ ns. The higher peak power of the faster implosions may possibly be attributed to a higher implosion velocity, which in turn improves the implosion stability, and/or to shorter wire ablation times, which may lead to a decrease in trailing mass and trailing current. Our results show that the scaling of the radiated x-ray peak power and total radiated x-ray energy scaling with peak drive current to be closer to quadratic than the results of Stygar *et al.* We find that the x-ray peak radiated power is $P_r\propto I^{1.57\pm0.20}$ and the total x-ray radiated energy $E_r\propto I^{1.9\pm0.24}$. We also find that the current scaling exponent of the power is sensitive to the inclusion of a single data point with a peak power at least 1.9σ below the average. If we eliminate this particular shot from our analysis (shot 1608), the power and energy scaling becomes closer to quadratic. Namely, we find that the dependence on the peak load current of the peak x-ray radiated power and the total x-ray radiated energy become $P_r\propto I^{1.71\pm0.10}$ and $E_r\propto I^{2.01\pm0.21}$, respectively. In this case, the power scaling exponent is different by more than 2σ from the previously published results of Stygar *et al.* Larger data sets are likely required to resolve this uncertainty and eliminate the sensitivity to statistical fluctuations in any future studies of this type. Nevertheless, with or without the inclusion of shot 1608, our results with $\tau_{\mathrm{imp}}=80$ ns fall short of an I^2 scaling of the peak x-ray radiated power by at least 2σ. In either case, the results of our study are consistent with the heuristic wire ablation model proposed by Stygar *et al.* ($P_r\propto I^{1.5}$). We also derive an empirical predictive relation that connects the power scaling exponent with certain array parameters.

DOI: 10.1103/PhysRevE.79.016412 PACS number(s): 52.25.Os, 52.77.Fv, 52.58.−c, 52.80.Vp

I. INTRODUCTION

Over the last few years a dramatic progress in applications of *z*-pinch x-ray sources driven by high voltage pulsed-power has been accomplished by using a new load architecture: Cylindrical wire arrays rather than cylindrical foils [1,2]. *z* pinches produced by the implosion of high wire number wire arrays and of high *Z* materials produced stable, reproducible and high x-ray radiated powers and energies and opened the path to consider *z* pinches as a promising and cost effective x-ray radiation source for indirectly driven inertial confinement fusion (ICF) research [3–6]. Wire-array *z* pinches produce peak x-ray powers that are larger than the electrical power driving the *z*-pinch implosions by a factor of 2 to 5.

Two of the crucial parameters of a pulsed-power driven *z*-pinch load, which determine in part the load x-ray yield, are the peak drive current and the time scale of the drive current. ICF goals such as fusion ignition or fusion yields >200 MJ, required for inertial fusion energy applications, define the needed x-ray power and energy and consequently define the driver's current and pulse length. It is therefore important to be able to predict the x-ray radiation yield of a future driver for a specific *z*-pinch load based on the accelerator design.

Systematic experiments at current levels of 1 to 20 MA, coupled with advanced diagnostics have recently shown that wire-array implosions are inherently three-dimensional during each of the several phases which describe its dynamics and evolution: Wire initiation, ablation, implosion, stagnation, and disruption [7–11]. However large scale two-dimensional (2D) and three-dimensional (3D) radiation magnetohydrodynamic *z*-pinch simulations are approaching a high level of maturity and may be able to reproduce some of the complex *z*-pinch dynamics and instability development

*National Nuclear Security Administration, Washington, DC 20585.

[12]. The current scaling results presented in this paper combined with integrated simulations of ICF capsule, x-ray source, and accelerator performance [5,6,13,14] will be used to define the system requirements.

With the exception of the most recent work [13,14], and the present study, previous current scaling experiments were performed in a noncontrolled way. The data presented in Refs. [15–17] were obtained with a number of different accelerators where the normalized pinch-current history was different. In addition, other critical pinch parameters such as the pinch material, initial array diameter, load electrode configuration, and implosion times were changed for each machine to optimize the radiation output energy. Furthermore, in some current scaling studies, results of gas-puff z pinches were included in the data. Therefore, the current scaling estimates deduced from those experimental works may not be physically valid in predicting the performance of a coupled pinch-driver system [14]. To deduce valid current scaling information, the experiments must be done in a controlled fashion. Normally only shots with the same accelerator and same load parameters must be included in the analysis. The only variable should be the current and by necessity the array mass. In this study we use the same accelerator for all different current value shots.

The compact 20-mm diameter, 10-mm long, 300 wire single-tungsten-wire array is widely used with the Z accelerator as a radiation source to drive the double-ended hohlraum ICF concept (see, for example, [4–6]). The originators of this concept were Hammer *et al.* [6]. The optimum mass for these compact arrays was assumed to be ~5.8 mg based on the criterion of maximizing the drive current from the Z accelerator, which would maximize the kinetic energy of the z-pinch implosion. The highest (90 kV) Marx charging voltage allowed at Z drives a maximum current of 19 MA through these heavy compact arrays, producing an implosion time of τ_{imp}=95 ns. The first systematic current scaling experiments were performed by Stygar *et al.* [13] at τ_{imp} =95 ns. That study measured a subquadratic radiated x-ray power (P_r) and energy (E_r) dependence on the peak load current (I), namely, $P_r \propto I^{1.24}$ and $E_r \propto I^{1.73}$. Later current scaling work by Nash *et al.*, [18] utilizing 40-mm diameter, 20-mm height, 240 wire, 4.6-mg tungsten-wire arrays with τ_{imp}=110 ns, measured a quadratic dependence of the radiated x-ray power on the peak load current (I) [18]. Wire ablation effects were proposed as a limiting factor in the power scaling with current at high wire-array mass [8,13]. Shorter implosion times were suggested as a means to improve wire-array performance by shortening the wire ablation time and possibly reducing trailing mass and current [8,13].

Recent experiments on Z were performed to evaluate the assumption that z-pinch x-ray performance would be optimum with the highest peak driving currents, e.g., at maximum implosion kinetic energy. Two "mass scans" or implosion time studies with the compact arrays were performed [19,20]. Experiments at τ_{imp}=65–67, 80–81, and 100–101 ns were performed and showed the highest radiated x-ray powers at τ_{imp}=80–81 ns (Fig. 1). The x-ray power was increased compared to heavier arrays, even though the peak drive current was reduced by ~2 MA. Furthermore, the highest radiation efficiency (power and/or current) was produced with τ_{imp}=67 ns at a peak current of about 13 MA [19]. The superior performance of lighter arrays with shorter implosion times motivated the present current scaling study at τ_{imp}=80 ns.

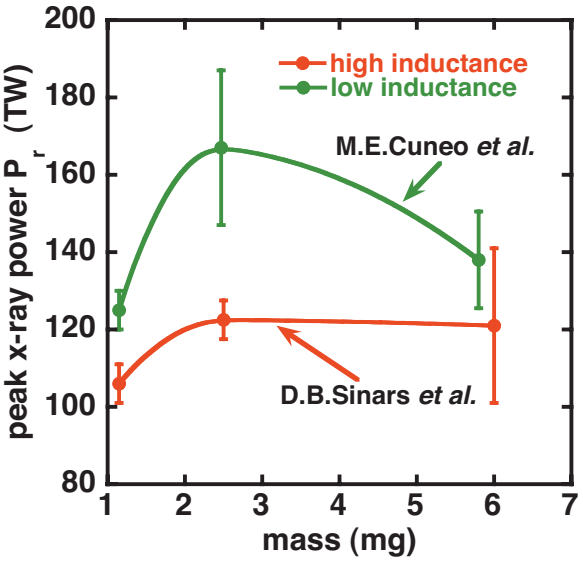

FIG. 1. (Color) This figure is compiled from data of Refs. [19,20] and includes unpublished data at 65 ns showing that 80 ns implosion time is the optimum.

The experimental arrangement is described in Sec. II. Measurements of the x-ray power, energy, rise time, and pulse width as a function of the peak load current are presented in Sec. III. In the same section the peak load current scaling functions of the above experimentally measured parameters are derived and presented. A discussion of our results comparing them to results expected from an ideal thin foil pinch is presented in Sec. IV. In Sec. V we compare our results with the heuristic model of Stygar *et al.* [13,14]. Utilizing the heuristic model we derive two scaling equations about the power scaling with the peak pinch current. Finally in VI we give a brief summary of our work.

II. EXPERIMENTAL ARRANGEMENT

The experiments presented in this paper were performed with the Z accelerator, which can drive up to a 20 MA current pulse within ~100 ns through a wire-array load. The Z-pulsed power design is based on the conventional Sandia pulsed power technology of Marx generators, water pulsed-forming and transmission lines, vacuum magnetically insulated transmission lines (MITL), and post-hole convolutes [21–29]. The oil and water sections contain 36 modules with identical components. The pulses of the 36 modules are combined together in parallel into four groups, with nine modules each, and feed four biconical constant impedance radial MITLs. The four pulses are then combined again in series via a double post-hole convolute section into a single ~20 MA, 2.5 MV pulse, which finally drives the z-pinch load on axis.

Based on the experiments discussed in [19,20], it appears that 80-ns implosion times obtained with 2.4 to 2.5 mg

single-tungsten-wire arrays produce higher peak powers than either the 5.8-mg or 1.15-mg arrays which pinch at 95 ns and 65 ns, respectively. Figure 1 compares peak powers for 65-, 80-, 95-, and 101-ns implosion times. Hence for our current scaling series we assumed the 2.5-mg total mass load as the optimum mass for the full, 90-kV Marx charge experiments. *Z* provided a peak current of 17 ± 0.3 MA. The current was decreased by decreasing the charging voltage to the lowest level that provided a stable *Z* accelerator operating point. At this lower charging voltage, 60 kV, the mass was adjusted to keep a constant 80-ns implosion time. This mass turned out to be of the order of 1.1 mg, the lightest 300 tungsten-wire array of 20-mm diameter ever utilized with the *Z* accelerator. The peak current provided by *Z* at 60 kV charge was about 11.2 ± 0.2 MA.

The SCREAMER code [30] was utilized with the experimentally adjusted *Z*-accelerator circuit model and the measured forward voltage wave forms. SCREAMER is a zero-dimensional (0D) circuit code developed as a design tool for pulsed power accelerators. It includes equivalent circuit models for accelerator and power flow components as well as a thin cylindrical shell implosion model. This model calculates and includes in the circuit the changing inductance of a current-driven collapsing thin shell. This is done by simultaneously solving the array equation of motion that determines the array inductance. A coupled equivalent circuit equation is used [16]. The SCREAMER calculations are provided only for reference. More detailed calculations including the effects of an ablation delay, plasma precursor injection, and snowplow accretion show energies within $\pm 10\%$ of a thin shell model without ablation when taken to the same convergence ratio (see Refs. [8,10] and especially [19]). So in the case of the ablation dynamics the velocity of the mass increases, but the mass at that velocity is lower, giving roughly the same kinetic energy (KE). This can also be understood in the following way: The work being done is the same; the pressure multiplied by the volume change is the same, to first order, independently of how the mass arrives at a particular radius. Moreover, the implosion times with ablation are within 1%–2% of those calculated without ablation.

Our study consists of 13 shots, five with ~1.1-mg and eight with ~2.5-mg mass. The tungsten-wire diameter for the 2.5-mg loads was approximately 7.4 μm. The 1.1-mg loads utilized a wire diameter of 5 μm. Figure 2 presents a side section of the load design and the final coaxial magnetically insulated transmission line (MITL) that transfers the total generator current into the load. In all our shots, except shots 1711 and 1735, we rigorously kept all the load hardware parameters the same, including wire number, array diameter and height, materials, and final transmission MITL anode cathode (*A*-*K*) gap. The anode cathode gap between the arrays and the return current cylinder (can) was 4 mm, while the gap of the final coaxial MITL was 3 mm. This was evaluated to be the optimum gap in previous experiments [13]. It was not too small to cause gap closure at peak load current and not unnecessarily large to increase the load inductance. Also, in order to have a direct comparison of our results with the previous current scaling work [13], we selected a load design exactly the same (Fig. 2). This way we could isolate the effect of the lighter masses and shorter implosion times on the current scaling law without any other parameter changes that could affect the experimental outcome. However, the results of the shots 1711 and 1735 were borrowed from another series of experiments done by Cuneo *et al.* [11]. Although the array geometry was identical to ours, the final feed section of the load hardware was slightly different: The final MITL was ~1 cm longer and conical, the viewing slots of the return current can were a bit wider (8 mm) to permit radiographic array imaging, also the radial gap between the wire array and the return current can was 3 mm larger (6 mm). However, the calculated inductance of the load was exactly the same as that of our current scaling series. We decided to use those two shots together with ours in order to increase the database and improve somewhat the statistics. In any case, the derived current power scaling law for the x-ray radiated power and energy remained exactly the same whether including or omitting those points in the analysis.

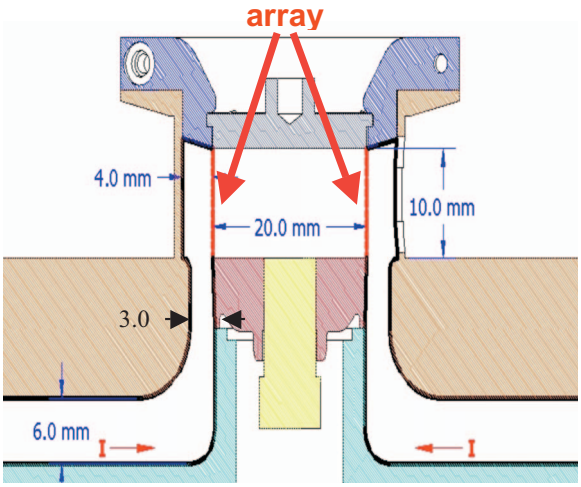

FIG. 2. (Color) Side section of the load design and the final coaxial self-magnetic insulated transmission line (MITL) that transfers the total generator current into the load.

The experiments of Ref. [13] and the present work used nearly an optimum number of tungsten wires based on previous wire number optimization experiments [31]. These experiments revealed that the optimum wire number for a 5.8 mg, 95-ns implosion time, 20-mm-diameter, 10-mm-long tungsten array was ~355. The peak x-ray power from this study shows a broad and relatively flat optimum between 250 and 450 wires. Assuming that the optimum wire number is related to the interwire spacing and to the wire expansion distance, and that the expansion distance is linearly related to the pulse length, we estimate that the optimum wire number for the 80-ns implosion times of the present study would be ~374. The current scaling experiments of Ref. [13] and the present work were performed with tungsten arrays of 300 wires.

To our knowledge, three current scaling campaigns have been performed under controlled conditions: The present series, the previous heavier 5.8-mg mass series [13], and the one of Ref. [18] where the load geometry was different than in both of the above series. In our measurements all the load parameters, dimensions, and material were strictly kept the

same for all of our shots as well as with those of the previous series of Ref. [13], except for the mass. Therefore, the difference of the current scaling laws discovered between the two campaigns can only be attributed to the mass itself and to the resulting shorter implosion times.

The return current cylindrical electrode which surrounded the wire array (Figure 2) had nine 5.6-mm wide slots (except for 1711 and 1735) around its center circumference corresponding to an equal number of lines of sights (LOS) where the various diagnostics observing the pinch were located. No axial diagnostics were utilized in the present series again in order not to introduce any variant relative to the previous campaign [13] which also did not have any hole at the anode electrode for observing the pinch axially from the top. We were concerned that the normally used 5-mm anode plate aperture [31] could introduce a difference in the array implosion and final stagnation on the axis [18].

The side LOS were oriented 12° above the pinch middle plane and contained among others a five channel x-ray diode (XRD) array [32], five diamond photoconducting detectors, three nickel bolometers integrating the radiated power during a 40-ns interval [33,34], and three microchannel plate pinhole cameras [35–37]. The latter were utilized to observe the radial evolution of the pinch as a function of time. Different pinhole sizes and filters were used to self-image the pinch in selected regions of the x-ray spectrum. The pinch power was determined by normalizing a spectrally equalized linear combination of the five XRD signals to the average of the 3-bolometer energy measurements [38]. The spatially integrated x-ray diagnostics observed only the upper one-half of the axial extent of the pinch, while the framing cameras recorded the entire length.

The load current was measured with two magnetic flux monitors (dB/dt) which were located at the anode side of the central biplate MITL [13], 6 cm away from the pinch axis and in almost diametrically opposite sides 150° apart [39,40].

III. EXPERIMENTAL RESULTS AND ANALYSIS

During the 13 shots we collected experimental results pertaining to the power, energy, rise time, full width at half maximum (FWHM), peak kinetic energy, and x-ray pinhole camera images of the pinch stagnation at the array axis. The apparent diameter of the stagnated plasma on the array axis was measured for a number of spectral ranges. We estimated the x-ray power and energy from the measurements assuming that the pinch was a Lambertian emitter for both the low and high current shots.

The main emphasis of this study is to establish the scaling of the peak radiated x-ray power and total x-ray radiated energy with the peak load current. We present in detail only the load currents, the power pulses, and energy measurements. Table I summarizes the load parameters and some of the experimental results. It contains the wire number, the wire diameters, the total load mass, the peak load current, the peak radiated x-ray power P_r, and the total radiated x-ray energy E_r, the 10%–90% x-ray power rise time τ_r, the effective x-ray power pulse width τ_w, which is defined as equal to E_r/P_r for the different peak pinch load currents, and the implosion time τ_i. For reference we also give the kinetic energy calculated by the SCREAMER thin-shell circuit model at a fixed, assumed convergence ratio of 10:1, and the fraction χ of the kinetic energy radiated as x-ray energy E_r. As noted previously, calculated yields including ablation are within ±10% (e.g., see Refs. [8,10,19]). These values are measured by identical instrumentation as the Ref. [13] study, and are defined in an identical fashion and calculated by identical algorithims to those in Refs. [13,14].

Figures 3 and 4 present normalized time-resolved samples of load current and x-ray power pulse measurements for both the low (blue color) and the high current (red color) cases. It is evident that the temporal variation of the currents and radiated x-ray power are very similar for the 17- and 11-MA shots. It is also worth noting that the load current continues to increase past pinch time to slightly higher value than before the pinch. This is characteristic of shorter implosion time pinches and signifies that not all the available driver energy is transferred to the load at pinch time. Furthermore, it may also signify current traveling in a lower inductance path across the power feed and/or as trailing current at larger radius in the z-pinch plasma itself.

Figures 5–8 depict the dependence of the P_r, E_r, τ_r, τ_w on the peak load current I. The following equations (1)–(4) summarize the current scaling dependence of the above parameters on the peak load current as derived from Figs. 5–8, with values taken from Table I,

$$P_r \propto I^{1.57\pm0.20}, \tag{1}$$

$$E_r \propto I^{1.9\pm0.24}, \tag{2}$$

$$\tau_r \propto I^{0.31\pm0.17}, \tag{3}$$

$$\tau_w \propto I^{0.30\pm0.19}. \tag{4}$$

In Figs. 5–8, the experimental points are equally weighted and least square fitted to a power law (solid line), with a zero intercept on the y axis. The uncertainties on the expressions (1)–(4) are the 1σ values of the fits.

Figures 9–13 compare our results with the previous work of Stygar *et al.* [13]. Figure 9 is an overlay of the current time history of Ref. [13] and the currents presented in Fig. 3. The current traces are again normalized, and the time scale of the ~95 ns shots of Ref. [13] is shortened in the proportion 80/95 in order to compare the normalized load current temporal evolution $f(t)$ of the two experiments. We may make several general observations in comparison to Ref. [13].

(1) Figure 9 suggests that the normalized load current temporal variation in both Ref. [13] and the present work is the same.

(2) The peak radiated power P_r is higher for $\tau_{\text{imp}}=80$ ns, increasing by 26% ± 7% on the average to 158 ± 26 TW from the 125 ± 24 TW obtained at $\tau_{\text{imp}}=95$ ns. The power increased even with a decrease of peak drive current from 18.8 ± 0.5 MA [13] to 17 ± 0.3 MA, confirming the trend noted with a somewhat different feed hardware in Ref. [19].

TABLE I. (a) Summary of load parameters and of some experimental results. (b) Summary of load parameters and of some experimental results.

(a)

Z-shot number	Number of wires n	Wire diameter (μ)	Total pinch mass m (mg)	Peak pinch current I (MA)	Peak x-ray power P_r (TW)	Total x-ray energy E_r (MJ)	X-ray power rise time τ_r (ns)
1143	300	4.79	1.04	11.1	80.0	0.54	3.1
1313	300	4.97	1.12	11.6	88.3	0.52	3.0
1605	300	4.80	1.04	11.1	77.6	0.59	2.5
1606	300	4.80	1.04	11.1	74.6	0.39	2.1
1607	300	4.80	1.04	11.0	84.1	0.54	3.0
Parameter averages of low current shots		4.83	1.06	11.2	80.9	0.52	2.7
Standard error		0.03	0.02	0.1	2.4	0.03	0.19
Sigma (σ)		0.08	0.04	0.2	5.4	0.07	0.43
1142	300	7.39	2.48	16.5	170.3	1.08	2.5
1312	300	7.41	2.50	16.7	139.8	0.86	3.2
1387	300	7.41	2.50	17.0	161.9	1.14	3.6
1414	300	7.41	2.44	17.2	198.0	1.32	2.8
1420	300	7.41	2.48	17.3	172.1	1.34	3.7
1608	300	7.41	2.50	17.1	107.9	0.77	3.1
1711[a]	300	7.30	2.42	16.7	152.6	1.43	3.1
1735[a]	300	7.30	2.42	17.1	159.1	1.17	2.8
Parameter averages of high current shots		7.38	2.47	16.95	157.7	1.15	3.10
Standard Error		0.02	0.01	0.10	9.3	0.08	0.14
Sigma (σ)		0.05	0.03	0.28	26.3	0.23	0.41

(b)

Z-shot number	Number of wires n	Total pinch mass m (mg)	X-ray power pulse width τ_w (ns)	Pinch implosion time τ_i (ns)	Pinch kinetic energy E_k (MJ)	Fraction of kinetic energy radiated χ
1143	300	1.04	6.7	79.5	0.206	2.62
1313	300	1.12	5.8	79.1	0.209	2.48
1605	300	1.04	7.6	79.2	0.206	2.86
1606	300	1.04	5.2	81.4	0.206	1.89
1607	300	1.04	6.4	80.8	0.206	2.62
Parameter averages of low current shots		1.06	6.4	80.00	0.210	2.49
Standard error		0.02	0.4	0.5	0.001	0.16
Sigma (σ)		0.04	0.9	1.0	0.001	0.36
1142	300	2.48	6.4	80.2	0.422	2.56
1312	300	2.50	6.1	81.3	0.424	2.03
1387	300	2.50	7.0	79.4	0.424	2.68
1414	300	2.44	6.7	81.0	0.418	3.16
1420	300	2.48	7.8	80.5	0.422	3.17
1608	300	2.50	7.2	82.3	0.424	1.82
1711[a]	300	2.42	9.4	80.0	0.416	3.43
1735[a]	300	2.42	7.3	79.2	0.416	2.81
Parameter averages of high current shots		2.47	7.1	80.5	0.421	2.71
Standard error		0.02	0.4	0.4	0.001	0.20
Sigma (σ)		0.05	1.0	1.0	0.004	0.56

[a]Shots 1711 and 1735 used different gaps and slot widths but had the same initial inductance.

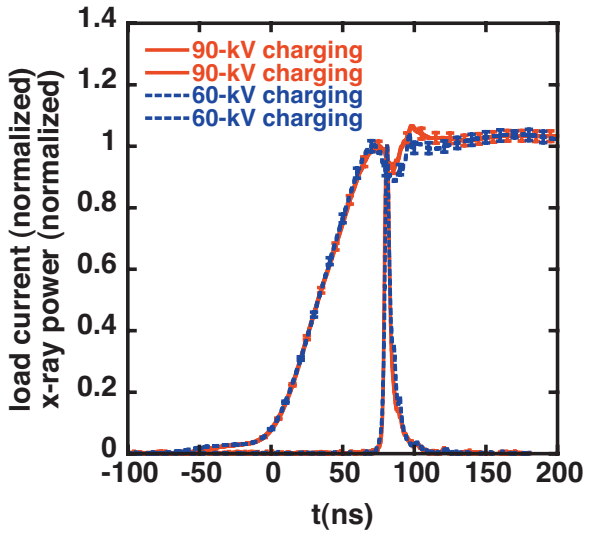

FIG. 3. (Color) Normalized time resolved samples of load currents for both the low (60-kV charging) and the high current (90-kV charging) cases. The normalized x-ray power pulses are also superimposed. The load current error bars represent statistical scatter of the curves and are equal to $\pm\sigma$.

(3) The P_r and E_r measurements scale closer to a I^2 dependence than the study performed at $\tau_{imp}=95$ ns, as discussed in more detail below. However, these scaling exponents for power, total energy, rise time, and pulse width overlap to within $\pm 2\sigma$ the results quoted by Stygar *et al.* for $\tau_{imp}=95$ ns, and may therefore be entirely consistent with that data set. This could be an artifact of the small numbers of experiments included in each data set. For example,

(a) The scaling exponents for power are larger than Ref. [13] but overlap to within 1.65 to 1.83σ.

(b) The scaling exponents for total energy overlap with Ref. [13] to within 0.67 to 0.89σ.

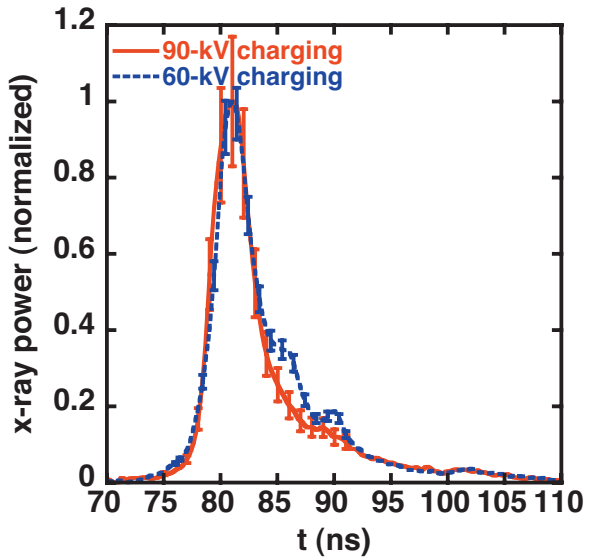

FIG. 4. (Color) Normalized time-resolved samples of radiated x-ray power pulses for both the low (60-kV charging) and the high (90-kV charging) current cases. The error bars represent statistical scatter of the curves and are equal to $\pm\sigma$.

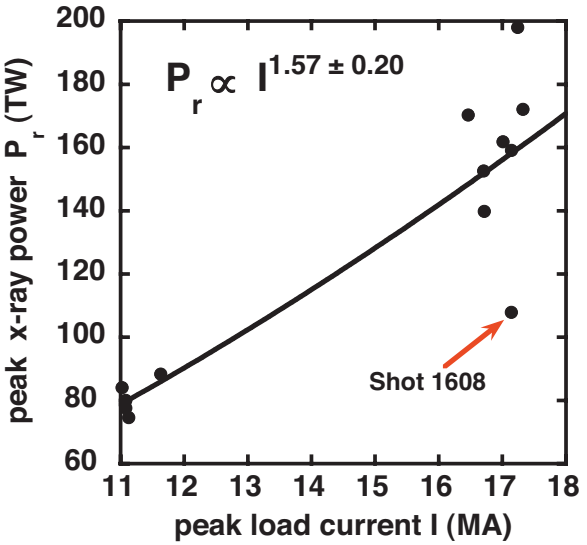

FIG. 5. (Color) Measurements of the peak radiated x-ray power P_r as a function of the peak load current I. The red arrow indicates the measurement of shot 1608 which might be excluded based on Chauvenet's criterion (see text and Ref. [43]).

(c) The scaling exponents for x-ray pulse rise time are weaker than Ref. [13] but overlap to within 0.24 to 0.50σ.

(d) The scaling exponents for x-ray pulse effective width are weaker than Ref. [13] but overlap to within 0.84 to 0.94σ.

(4) The τ_r and τ_w scalings in the present data are equivalent to a small variation almost independent of the peak current I. The rise time and effective pulse width of the x-ray pulse τ_r and τ_w are smaller and proportional to each other. Namely, for both our high and low currents shots, the effective pulse width τ_w is approximately 2.3 times the rise time τ_r. They also have practically the same scaling with the peak

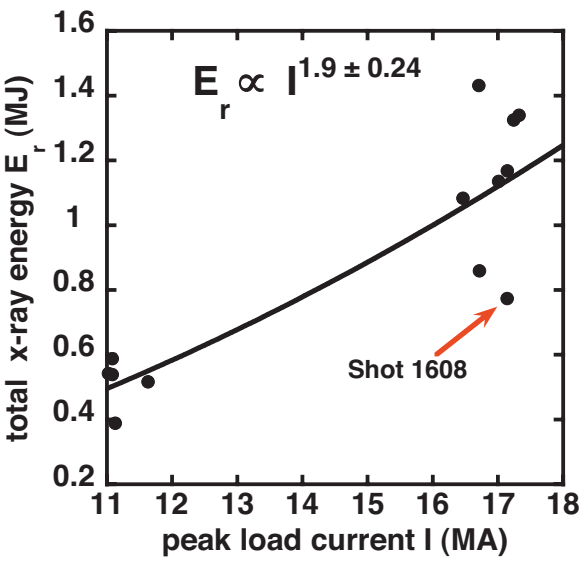

FIG. 6. (Color) Measurements of the total radiated x-ray energy E_r as a function of the peak load current I. The red arrow indicates the measurement of shot 1608 which might be excluded based on Chauvenet's criterion (see text and Ref. [43]).

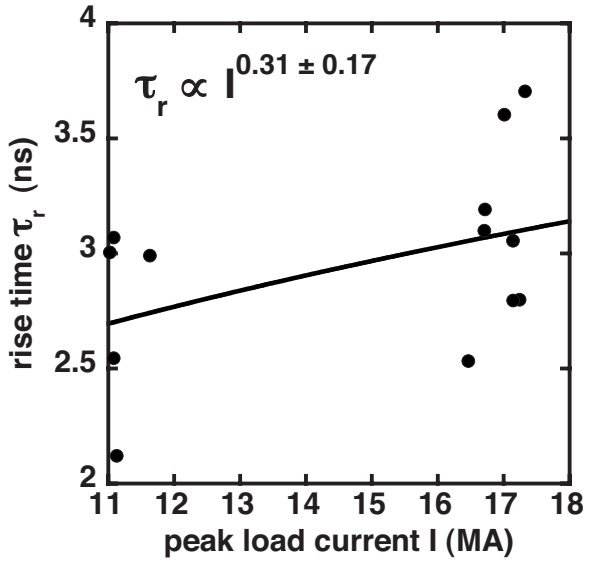

FIG. 7. Measurements of the 10%–90% x-ray-power rise time τ_r as a function of the peak load current.

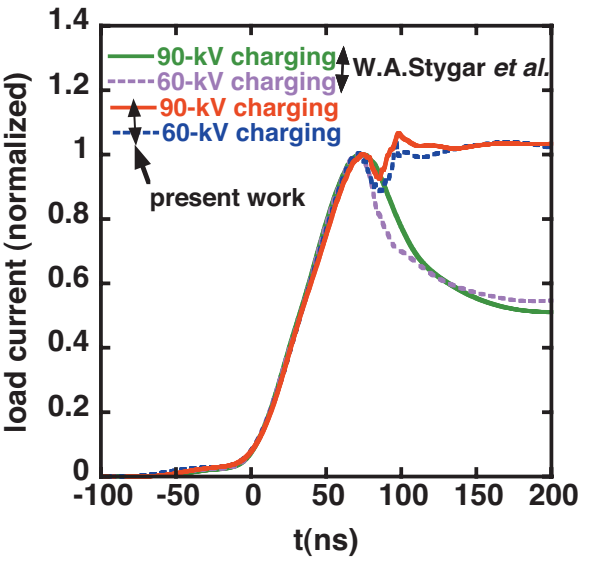

FIG. 9. (Color) Time history of the normalized currents of the present experiments compared with those of Ref. [13]. The time scale for the 95 ns shots of Ref. [13] is shortened by the ratio 80/95. The time history appears to be the same for both works.

load current (Figs. 7 and 8). So the higher power of the shorter implosion time arrays may be due to less instability growth during the implosion for wire arrays with higher acceleration and higher implosion velocity [41,42].

(5) The total radiated energy is lower, consistent with the lower drive currents.

We also find that the current scaling exponent for peak power is sensitive to the statistical excursions in the data, whether through the natural statistical fluctuations in the data or through possible uncontrolled (and unknown) variations in some of the experiments. This sensitivity may be an artifact of a small sample size (13 shots in this study, 15 shots in Ref. [13]). For example, from Table I, we find that shot 1608 is 1.893σ lower than the average power at the 17-MA level calculated including shot 1608 ($P_r = 157.7 \pm 26.3$ TW). Such an excursion would be expected once every 17 shots if the process followed a Gaussian or normal probability distribution. We have a sample of only eight shots at high current. The probability to have shots with at least a 1.893σ deviation [43] is 5.88%. Therefore, for eight total shots at high current that we fired we should expect $8 \times 0.0588 = 0.47$ shots to have a deviation from the average at least 1.893σ. According to Chauvenet criterion [43], if the expected number of measurements which are at least as deviant as the suspected measurement is less than one half, then the suspected measurement might be considered for rejection. Therefore, we could have reasonable justification to reject shot 1608 and adopt $P_r \propto I^{1.71 \pm 0.10}$ as the radiated x-ray power scaling. If we cal-

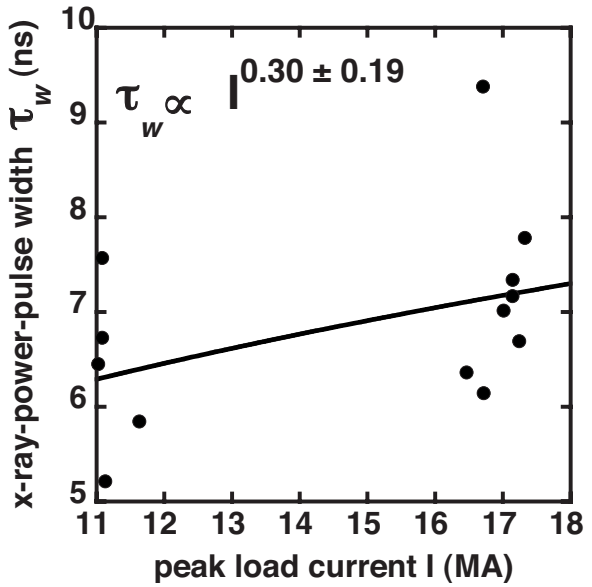

FIG. 8. Measurements of the effective x-ray-power-pulse width $\tau_w \equiv E_r / P_r$ as a function of the peak load current.

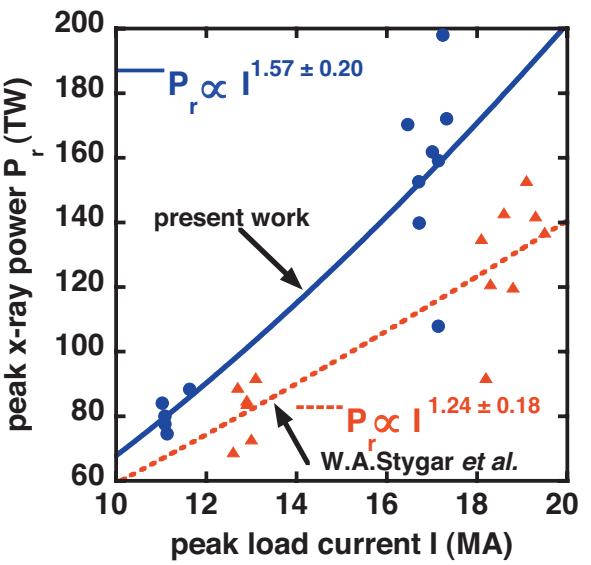

FIG. 10. (Color) Comparison of our peak radiated x-ray power P_r measurements with those of Stygar *et al.* [13].

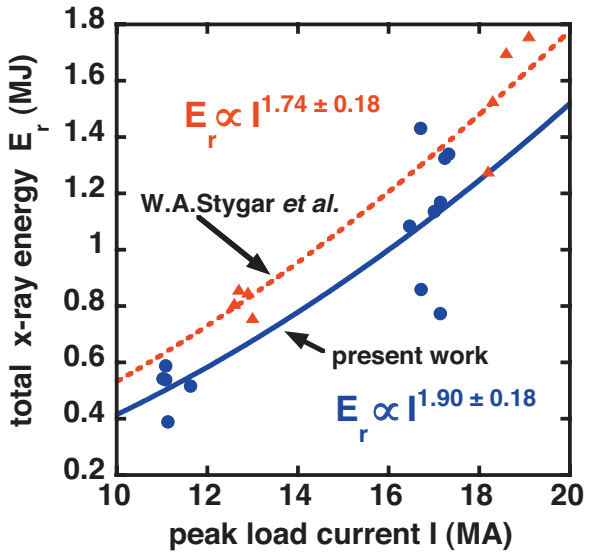

FIG. 11. (Color) Comparison of our total radiated x-ray energy E_r measurements with those of Stygar *et al.* [13].

culate the average power at 17 MA excluding shot 1608 ($P_r = 165 \pm 18$ TW), we find that shot 1608 is equivalent to a 3.2σ excursion. In Figs. 14 and 15 we depict the scaling derived if shot 1608 is excluded. The power and energy scaling are closer to quadratic, while the τ_r, and τ_w scaling with peak load current remains practically the same as in Figs. 7 and 8. Figure 16 compares the three power fits; the top fit excludes shot 1608 (blue points and line), the middle fit (green broken line) includes all shots, and the lower fit (red broken line and red points) represents the results of Ref. [13]. The 1608 power measurement is shown as a green oversized square.

Hence if we exclude shot 1608, the power fit for the radiated x-ray power (Figs. 14 and 15) comes closer to quadratic, while for the energy it becomes exactly quadratic, namely,

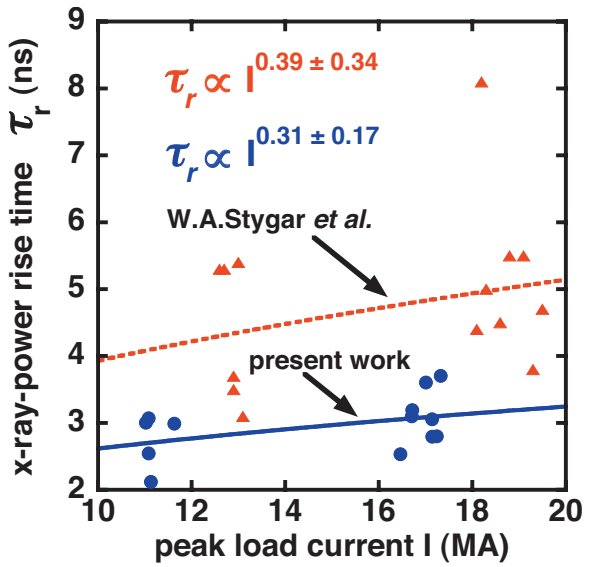

FIG. 12. (Color) Comparison of our 10%–90% x-ray-power rise time τ_r measurements with those of Stygar *et al.* [13].

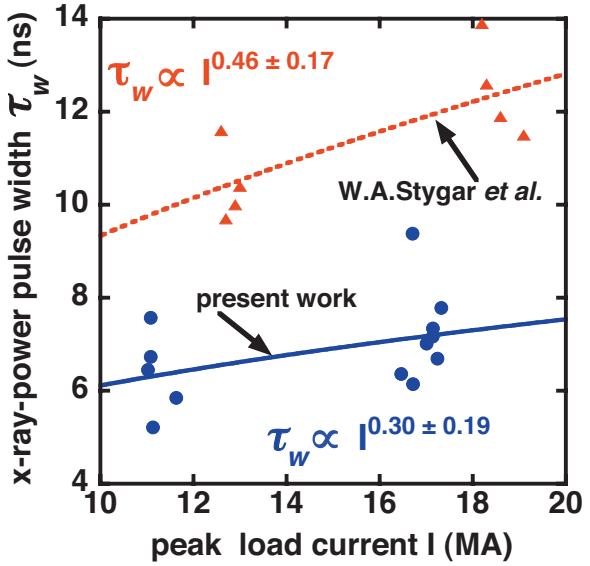

FIG. 13. (Color) Comparison of our effective x-ray-power-pulse width $\tau_w \equiv E_r / P_r$ measurements with those of Stygar *et al.* [13].

$$P_r \propto I^{1.71 \pm 0.10}, \tag{5}$$

$$E_r \propto I^{2.01 \pm 0.21}. \tag{6}$$

The scaling of power with current without shot 1608 is different from the results of Ref. [13] by 4.7 to 2.6σ, and may therefore not be consistent with that data set. Resolution of this matter therefore impacts our interpretation of this experiment and remains an uncertainty. The power scaling however, with or without shot 1608, still excludes quadratic scaling to 2σ, the level typically used to determine if a result is statistically significant [43].

IV. DISCUSSION OF THE RESULTS

If the pinches of the wire arrays could be considered as similar to those of infinitely thin and stable cylindrical foils,

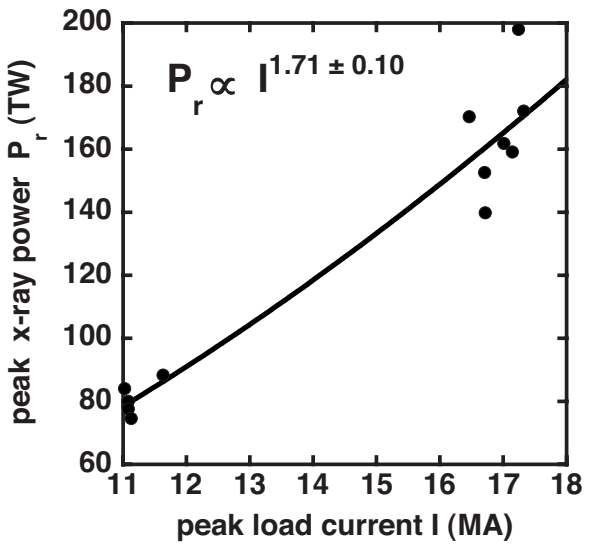

FIG. 14. Peak radiated x-ray power P_r current scaling fit without 1608 shot results.

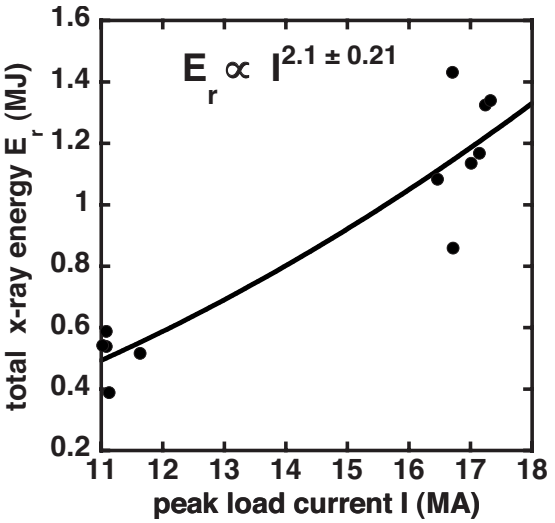

FIG. 15. Total radiated x-ray energy E_r current scaling fit without 1608 shot results.

imploding under the forces of the azimuthal magnetic field generated by the uniform current flowing through them, then the implosion force, the pinch time, and the foil kinetic energy could be expressed as follows [13,14]:

$$\frac{\mu_0 \ell I^2 f^2(t)}{4\pi} = -mr(t)\frac{d^2 r}{dt^2}(t), \tag{7}$$

$$\tau_i \equiv \int_b^a \frac{dr}{v(r)}, \tag{8}$$

$$E_k(r) \equiv \frac{1}{2}mv^2(r) = \frac{-\mu_0 \ell I^2}{4\pi}\int_b^r \frac{F^2(r)dr}{r}, \tag{9}$$

where μ_0 is the free-space magnetic permeability, ℓ is the axial length of the pinch, I is the peak pinch current, $f(t)$ is the normalized pinch current as a function of time, m is the pinch mass, $r(t)$ is the pinch radius as a function of time, τ_i is the pinch-implosion time, b is the initial pinch radius, a is the final pinch radius, $v(r)$ is the pinch velocity as a function of r, $E_k(r)$ is the pinch kinetic energy as function of r, and $F(r)$ is the normalized pinch current as a function of r, where $F[r(t)] \equiv f(t)$. (Equations are in SI units throughout.) We define a to be the effective radius at which the pinch stagnates and its kinetic energy is thermalized.

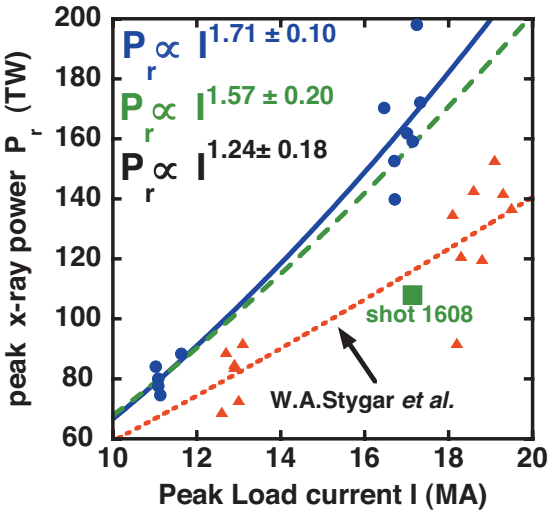

FIG. 16. (Color) This figure compares three fits; the top fit excludes shot 1608 (blue points and line), the middle fit (green broken line) includes all shots, and the lower fit (red broken line and red points) represents the results of Ref. [13]. The 1608 power measurement is shown as a green oversized solid square.

Although our experiments utilized very light masses and a considerable number of wires (300), still the interwire gaps were not so small for the arrays to be considered as cylindrical foils and not so thin as to approach the pinch conditions described by Eqs. (7)–(9) which from this point on we will call the "ideal pinch." For example, measurements show that the wire ablation periods for the τ_{imp}=80 and τ_{imp}=95 ns arrays are 60% of the implosion time and equal to 50 and 60 ns, respectively [8,10,11]. However, in order to gain better insight into our results, we compare them with the behavior of an ideal pinch. According to the previously described equations and Refs. [13,14], in order to have a quadratic scaling dependence of the radiated x-ray energy and power with the peak load current, five conditions must be fulfilled, under the assumptions that the total radiated energy is proportional to E_k [13,14]:

(a) The time dependence of the normalized pinch current $f(t)$ must be independent of the actual current amplitude.

(b) The same must be true for the radial dependence of the current $F(r)$.

(c) The thermalization times must be again independent of the current.

(d) The size of the emission region at stagnation should be the same.

(e) Finally, the fraction of the array kinetic energy at stagnation which is thermalized and radiated as x rays must be independent of the current I.

Let us now see how close our experimental results come to fulfilling these conditions.

Figure 3 overlays the normalized load current for the 17-MA and 11-MA runs. They are almost identical. This of course satisfies condition (a). Figure 17 compares the effective high and low current radii as a function of time. Figure 18 compares the normalized pinch currents as a function of the radius as the array implodes to pinch. These radial dependences of the current were obtained by unfolding the inductance variations of the imploding wire array assuming that resistance is negligible [44]. Both traces overlap satisfactorily well. There are some differences at the small radius section near pinch times where the unfolding technique gives a somewhat larger weight to smaller amounts of currents flowing at larger radii. It appears that for the 1.1 mg shots (low current) there is less of the current flowing at larger radii at pinch times. This is suggestive of a tighter pinch for the lower current case. A closer look at the normalized current data of Fig. 9 reveals that the 60 kV load current traces, for 80 ns and 95 ns, have a slightly faster inductive dip after peak current (see also Fig. 3). Figure 19 corroborates this observation. Aside from the slight differences in the small radii, the load current radial dependence for both low and high current traces are very close to being the same, and

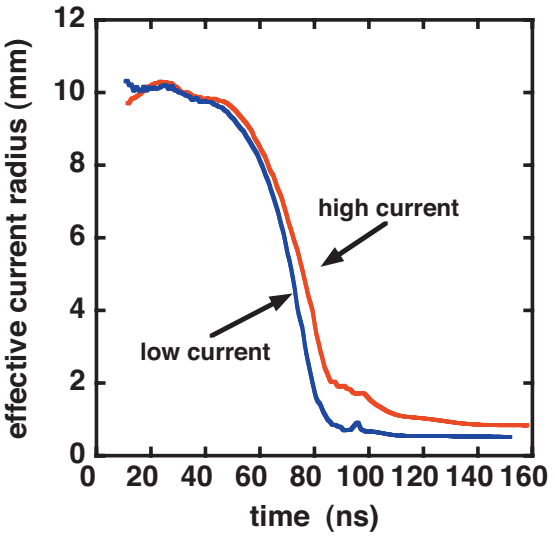

FIG. 17. (Color) Comparison by overlaying the effective current radius of both a high and a low current shot as a function of time.

therefore we conclude that condition (b) is approximately satisfied.

Figure 4 is an overlay of the x-ray power radiated pulse. The rise times for both low and high current cases are almost identical and approximately equal to 3 ns. Figure 7 also shows that the average increase in the rise time τ_r going from the lower to higher currents is 0.4 ns. The average rise time for the high current case is 3.1 ± 0.4 ns, while for the lower current case is 2.7 ± 0.4 ns. This is a $15\% \pm 3\%$ increase in rise time for the high current case compared to low current. The observed radiated energy scales close to the total available energy which scales as $I^2 \sim (17/11.2)^{1.9} \sim 2.2 \pm 0.1$. If the thermalization times were the same for the low and high

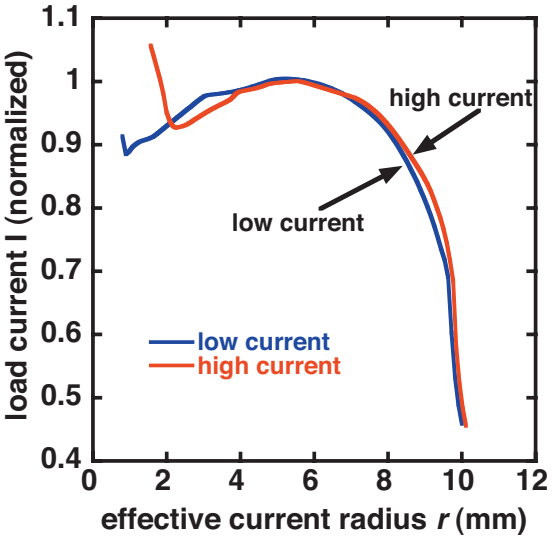

FIG. 18. (Color) Comparison by overlaying the normalized pinch current as a function of the radius as the array implodes to pinch. These radial dependences of the current were obtained by unfolding the inductance variations of the imploding wire array [43]. These results are similar to those of Ref. [43], e.g., lower current case pinches a little tighter.

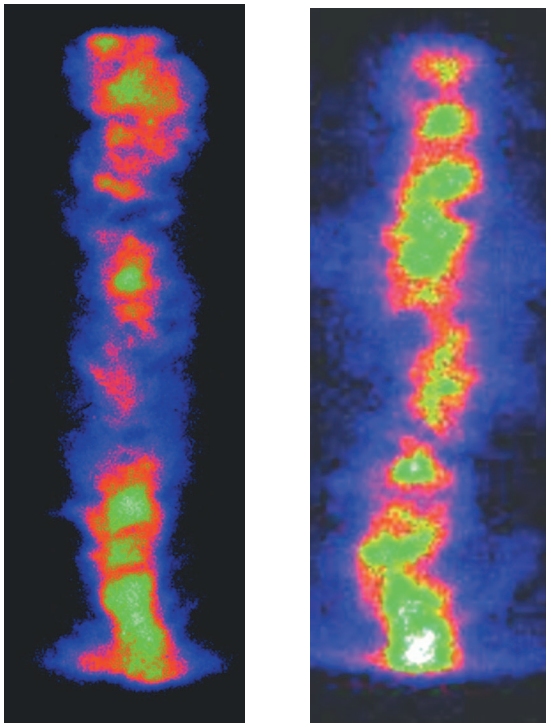

FIG. 19. (Color) X-ray images of the entire pinch length at pinch time for the low current (60-kV charging of the Marx generators) (left-hand side) and for the higher current (90-kV charging of the Marx generators) (right-hand side). The images represent a 3.9 mm × 8.5 mm field of view. The time exposure was 2 ns. The spectrum cutoff was approximately 200 eV. The distance listed beneath is the full width at half-maximum of the pinch obtained by integrating the image in the axial direction. The diameter of the pinch at stagnation is larger for the higher current by 0.29 mm.

currents, (i.e., the times it takes to convert the work done on the pinch into electron thermal and then excitation energy) then the high current shots should radiate $\sim 2.2 x P_{\text{low}}$ ($P_{\text{low}} = 81$ TW), which is ~ 180 TW. The measurements show that the average $P_{\text{high}} \sim 160$ TW, a 13% reduction compared to the ideal case, which is quite similar to the increase of the rise time.

Furthermore, the average spectrally equalized linear combination of the five XRD x-ray pulse geometric FWHM is $\tau_{\text{FWHM}} = 4.17 \pm 0.15$ for the high current shots and $\tau_{\text{FWHM}} = 3.95 \pm 0.59$ for the low current shots, a $5\% \pm 1\%$ decrease. The average effective widths of the x-ray radiated pulse are higher for the high current ($\tau_w = 7.1 \pm 1$) than for the lower current ($\tau_w = 6.4 \pm 0.9$) by $11\% \pm 2\%$. Since $P_r \sim E_r / \tau_{th}$, it appears that the rise time τ_r and the effective width τ_w come closer to being proportional to thermalization times than the geometric FWHM τ_{FWHM}, since the low to high current rise time τ_r variation ($15\% \pm 3\%$) and the effective width τ_w variation ($11\% \pm 2\%$) are approximately the same as the average power variation (13%). Condition (c) therefore falls short by 10% to 15% from being completely fulfilled.

The profile of our pinches at stagnation are less fragmented and approximately one-half the size of those in Ref. [13]. However, the diameter of the emission region at stagnation is larger for the higher current by 0.29 mm (Fig. 19). The observed convergence ratios of the low and high currents are, respectively, 10:0.48 and 10:0.625, larger than the assumed 10:1 in our SCREAMER calculations. This makes the high current pinch diameter 30% larger, which is in the same direction as the rise times (15% larger), effective widths (11%), or power variations (13%). Therefore, the size of the higher current pinch deviates from the ideal case by 23%. Hence condition (d) falls short by 23% from being completely fulfilled.

In addition to the experimental results, Table I includes the kinetic energy for every shot as calculated by the thin-shell circuit code SCREAMER at an assumed radial convergence ratio of 10:1. The SCREAMER calculations are provided only for reference. More detailed calculations including the effect of an ablation delay, plasma precursor injection, and snowplow accretion show energies within ±10% of a thin shell model when taken to the same convergence ratio (see Refs. [8,10], and especially [19]). The ratio of the radiated total energy versus the kinetic energy is presented in the last column of the Table I as the parameter χ. There is some variation from shot to shot similar, of course, to that of the total radiated energy (Fig. 6). However, (and this is significant for our analysis), the average value of χ for the low current shots (2.5 ± 0.4) is quite close to the average value of χ (2.7 ± 0.6) for the high current shots. Now if the total work performed by the $\boldsymbol{j} \times \boldsymbol{B}$ forces on the pinch is proportional to the calculated 0D kinetic energy E_k, then one could conclude that the fraction of the kinetic energy thermalized and radiated as x rays is practically independent of the peak pinch current [condition (e)]. In all our z-pinch work throughout the years we have found that the total x-ray radiated energy is at least 2 times the ion kinetic energy as calculated using a 0D pinch model that assumes (i) an infinitely thin and perfectly stable imploding foil, and (ii) that no more $\mathbf{j} \times \mathbf{B}$ work is performed on the infinitely thin and stable foil after it reaches a final radius. Although the pinch kinetic energy obtained from 0D and one-dimensional (1D) calculations is substantially less than the measured radiated x-ray energy, such a discrepancy does not exist for the more accurate 2D calculations [45]. According to the 3D MHD simulations performed by Chittenden *et al.* [12], the total radiated energy E_r is, to a good approximation, equal to the total work performed by the $\mathbf{j} \times \mathbf{B}$ force on the pinch plasma. (Please see page B464 and Fig. 5 of the Chittenden reference [46].) This result is identical to that obtained by the 2D MHD simulations performed by Peterson, who also find that the total radiated energy E_r is, to a good approximation, equal to the total work performed by the $\mathbf{j} \times \mathbf{B}$ force on the pinch plasma. Hence in summary this apparent discrepancy is due to the fact that the 0D SCREAMER model assumes that no more work is performed by the $\mathbf{j} \times \mathbf{B}$ force after the imploding thin foil shell has reached the preimposed minimum radius (in our case 1 mm with 10:1 convergence ratio).

Based on the above considerations of the conditions (a), (b), (c), (d), and (e) one could expect our pinches to be close to but not perfectly ideal. By "perfectly ideal" we remind the reader that we refer to the implosion of an infinitely thin cylindrical foil imploding without any instability under the azimuthal magnetic forces described in Eqs. (7)–(9). This appears to be the case. As shown by the power fits of Figs. 5 and 6, the scaling for our data are closer to quadratic than the heavier mass data [13]. However our results do exclude quadratic dependence of power scaling to 2σ, similar to the conclusions of Ref. [13] at $\tau_{\mathrm{imp}}=95$ ns, with or without the inclusion of shot 1608.

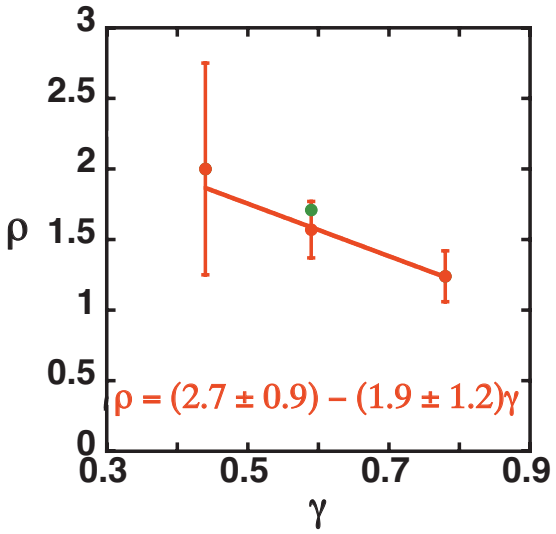

FIG. 20. (Color) Universal graph that relates the right-hand side of the expression (10) $[\frac{\delta_a}{\delta_{\mathrm{RT}}} \propto (\frac{m}{\ell})^{1/4} \frac{1}{(R\Gamma)^{1/2}}]$ (which for ease of representation we call it here γ) with the peak load current exponent ρ. The green color point has a $\rho=1.71$ and corresponds to the x-ray radiated power current scaling exponent when we do not include shot 1608 (present work).

As derived from our experimental results it is clear that the lighter, 2.5 mg, $\tau_{\mathrm{imp}}=80$ ns arrays yield a higher radiated power and a tighter and better quality z pinch at stagnation from comparison to Ref. [13] (Fig. 20). These results are consistent with the trends shown in [19]. There are a number of possible hypothesis for the improvement of power. The improvement may arise in part because higher accelerations with lighter arrays (the shorter implosion times give higher implosion velocities) are less susceptible to the development of the magneto-Rayleigh-Taylor instability [41,42]. It is also possible that the amount of mass that trails behind the fastest implosion front is decreased [8], and this may allow more of the current to flow at a smaller radius which results in a more energy efficient and tighter pinch [8,44].

In Ref. [13] it was demonstrated via an analytic model that the current scaling results were not affected by the increase of the internal energy and radiative opacity as the load mass and current were increased. However, at least some of the increase in radiated power for the lighter arrays relative to the heavier may therefore also result from a 60% decrease in the internal energy of the hot tungsten plasma. These questions will be a subject for future work.

The question of whether the power scales more favorably with current for $\tau_{\mathrm{imp}}=80$ ns compared to $\tau_{\mathrm{imp}}=95$ ns does depend on the inclusion of shot 1608. We found that with

shot 1608 the scaling exponent for power is within 1.65 to 1.83σ of those shown in Ref. [13]. Without shot 1608 the scaling exponent for power differs from the results of [13] by 2.6 to 4.7σ. This question will require further investigation.

V. COMPARISON OF OUR RESULTS WITH PROPOSED SCALING MODELS

We compare our results with the theory and scaling relations derived by Stygar *et al.* in Refs. [13,14]. According to those papers we can predict when the implosion dynamics are dominated either by ablation effect or RT by examining the ratio of δ_a to δ_{RT}:

$$\frac{\delta_a}{\delta_{\mathrm{RT}}} \propto \left(\frac{m}{\ell}\right)^{1/4} \frac{1}{(R\Gamma)^{1/2}}. \tag{10}$$

If $\delta_\alpha/\delta_{\mathrm{RT}}$ is larger than unity we have ablation-dominated pinch while when $\delta_\alpha/\delta_{\mathrm{RT}}$ is smaller than unity we have an RT-dominated pinch. Where δ_a is the characteristic radial thickness of the imploding wire-array plasma, assuming that the RT instability and other sheath-broadening mechanisms can be neglected. On the other hand, δ_{RT} is the characteristic radial thickness of the imploding wire-array plasma when the ablation effects are assumed negligible and the sheath thickness is caused solely by the Rayleigh-Taylor (RT) instability. In expression (10), m is the total wire-array mass expressed in mg, ℓ is the axial length of the array in cm, and R is the initial array radius in cm. The parameter Γ can be estimated from experimental values by the expression

$$\Gamma = \frac{\tau_i I}{R}\left(\frac{\mu_0 \ell}{2\pi m}\right)^{1/2}, \tag{11}$$

where τ_i is the implosion time, I is the peak load current, and μ_0 the magnetic permeability of free space which is equal to $4\pi \times 10^{-7}$. Equation (11) is in SI units, and Γ is dimensionless. The function Γ is directly related to the dimensionless parameter $\Pi = \frac{m_0 I^2 \tau_{\max}^2 \ell}{4\pi m R^2}$, first introduced by Ryutov *et al.* [42], with the difference that Π is a function of the time ($\tau_{\max}$) where the load (I) current reaches maximum. If we replace $\tau_{\max}$ in Π with τ_I, Π becomes equal to $\Gamma^2/2$.

In addition, further guidance on whether the RT or ablation dominates the current scaling results is given by the following two expressions derived in Ref. [14]: If the pinch mechanism is ablation dominated, then the x-ray radiated power scales as the 3/2 power of the load current,

$$P_r \propto \left(\frac{I}{\tau_i}\right)^{3/2}. \tag{12}$$

However, if the RT instability dominates the pinch, then the power scaling is quadratic with the peak load current I,

$$P_r \propto \frac{I^2}{\tau_i}. \tag{13}$$

The above expressions assume that the R and ℓ for the set of current scaling experiments is kept the same. This scaling was first derived in Ref. [42] by Ryutov *et al.* with the difference that $\tau_{\max}$ (the time to maximum load current I) was utilized instead of τ_i.

Table II gives a summary of the values of Γ and expression (10) based on the experimentally measured parameters, which are also shown in the first few columns. Γ is approximately constant for all our shots with an average value of 3.89 ± 0.02. The expression (10) is smaller than 1 and varies between an average value of (0.514 ± 0.05) for our lower mass shots to (0.636 ± 0.07) for the higher mass shots with an overall average of 0.59 ± 0.06.

The experimental results of Ref. [18] with a circular viewing aperture in the anode electrode demonstrated a quadratic dependence. This signifies that the pinch may have been RT dominated. The values of expression (10) varied between (0.40) and (0.48) with an average of 0.44. Taking into account all the above three sets of current scaling experimental campaigns (Refs. [18,13], and present work), we can suggest that when expression (10) is ~0.4 [18] or lower we have RT dominated pinches. Again when expression (10) is 0.78 ± 0.08 (experiments of Ref. [13]) we postulate an ablation-dominated implosion mechanism. If we call the right-hand side of expression (10) γ and the proportionality function of expression (10) $K(\gamma)$, then the expression (10) becomes

$$\frac{\delta_a}{\delta_{\mathrm{RT}}} \equiv K(\gamma)\left(\frac{m}{\ell}\right)^{1/4} \frac{1}{(R\Gamma)^{1/2}}. \tag{14}$$

Based on the present experiments and those of Ref. [13] we can say with certainty that the proportionality function $K(\gamma) > 1$ $(\mathrm{kg/m^3})^{-1/4}$ in order that the current scaling series of Ref. [13] be ablation dominated ($\frac{\delta_a}{\delta_{\mathrm{RT}}} > 1$). All of the experiments of the present work and of Refs. [13,14] have a γ,

$$\gamma = \left(\frac{m}{\ell}\right)^{1/4} \frac{1}{(R\Gamma)^{1/2}} < 1 \ (\mathrm{kg/m^3})^{1/4}, \tag{15}$$

with the maximum of 0.8 $(\mathrm{kg/m^3})^{1/4}$ (Ref. [13]) and minimum 0.4 $(\mathrm{kg/m^3})^{1/4}$ (Ref. [18]). Since measurements with $\gamma \sim 0.8$ $(\mathrm{kg/m^3})^{1/4}$ appear to be "ablation dominated" ($P_r \propto I^{3/2}$) and experiments with $\gamma \sim 0.4$ $(\mathrm{kg/m^3})^{1/4}$ RT dominated ($P_r \propto I^2$), then the value of $K(\gamma)$ must vary between the following values:

$$1.25 \ (\mathrm{kg/m^3})^{-1/4} < K(\gamma) < 2.5 \ (\mathrm{kg/m^3})^{-1/4}. \tag{16}$$

For values of γ between 0.8 $(\mathrm{kg/m^3})^{1/4}$ and 0.4 $(\mathrm{kg/m^3})^{1/4}$ both mechanisms, RT and ablation, substantially contribute to the pinch behavior with the ablation effects decreasing as the γ approaches the value of 0.4 $(\mathrm{kg/m^3})^{1/4}$. Of course, the above conclusions are phenomenological and are based on our interpretation of the experimental results.

Our data with an average value of $\gamma = 0.59$ $(\mathrm{kg/m^3})^{1/4}$ should be closer to quadratic scaling than the data of Ref. [13] that have a $\gamma = 0.8$ $(\mathrm{kg/m^3})^{1/4}$. Indeed this is the case. However, based on this phenomenological argumentation, we conclude that the pinch power scaling is influenced by wire ablation effects although possibly less significantly than the longer implosion time experiments described in previous work [13].

TABLE II. Summary of the values of parameter Γ and of the expression $\delta_a/\delta_{RT} \propto (m/\ell)^{1/4} 1/(R\Gamma)^{1/2} \equiv \gamma$ (10) based on the experimentally measured parameters which are also shown in the first few columns.

Z-shot number	Axial pinch length ℓ (mm)	Initial wire-array radius R (mm)	Number of wires n	Total pinch mass m (mg)	Peak pinch current I (MA)	Pinch implosion time τ_i (ns)	Γ_{exp}	$(m/\ell)^{1/4} 1/(R\Gamma)^{1/2}$
1143	10	10	300	1.04	11.1	79.5	3.87	0.51
1313	10	10	300	1.12	11.6	79.1	3.88	0.52
1605	10	10	300	1.04	11.1	79.2	3.85	0.51
1606	10	10	300	1.04	11.1	81.4	3.96	0.51
1607	10	10	300	1.04	11.0	80.8	3.90	0.51
Parameter averages of low current shots				1.06	11.2	80.0	3.89	0.512
Standard error				0.02	0.1	0.5	0.19	0.002
Sigma (σ)				0.04	0.2	1.0	0.42	0.004
1142	10	10	300	2.48	16.5	80.2	3.76	0.65
1312	10	10	300	2.50	16.7	81.3	3.84	0.64
1387	10	10	300	2.50	17	79.4	3.82	0.64
1414	10	10	300	2.44	17.2	81.0	3.99	0.63
1420	10	10	300	2.48	17.3	80.5	3.95	0.63
1608	10	10	300	2.50	17.1	82.3	3.98	0.63
1711	10	10	300	2.42	16.7	80.0	3.84	0.64
1735	10	10	300	2.42	17.1	79.2	3.89	0.63
Parameter averages of high current shots				2.47	16.95	80.5	3.88	0.63
Standard error				0.01	0.10	0.4	0.029	0.003
Sigma (σ)				0.03	0.28	1.0	0.083	0.007

Another more straightforward way of fitting the x-ray radiated power scaling ρ with the peak load current is the universal graph of Fig. 20, which relates γ with the exponent ρ of the peak load current through the expression

$$\rho = (2.7 \pm 0.9) - (1.9 \pm 1.2)\gamma. \quad (17)$$

Hence if we fire only one shot and measure τ_i and I, then from the load parameters of Table I and Fig. 17 we may estimate the x-ray radiated power scaling ρ and consequently whether the pinch dynamics will be RT or ablation dominated. To make Fig. 20 we utilized the experimentally derived values of ρ and γ from the present work and Refs. [13,18].

It appears to us that the heuristic model of Stygar *et al.*, is in agreement with our results (with or without the inclusion of shot 1608) and may therefore suggests that our data have a substantial contribution of ablation to the instability-induced width of the imploding plasma. This is an interpretation of the above model. This is also a prediction to be compared with future detailed measurements of the radiographically measured shell width [19].

VI. SUMMARY

In summary, our results demonstrate that lighter masses and shorter implosion times produce much better pinches as witnessed by faster x-ray pulse rise times, the tighter pinches shown by the x-ray framing cameras (Fig. 19), the smaller FWHM of the radiation pulse, and of course the higher peak radiated power.

Despite the fact that those pinches approached the "ideal pinch" [the pinch of an infinitely thin foil imploding without any instability as described by Eqs. (7)–(9)], the radiated power current scaling still falls short of the quadratic ($P_r \propto I^{1.57\pm0.20}$ to $P_r \propto I^{1.71\pm0.10}$) but nevertheless remains closer to ideal than one with heavier masses and ~95 ns implosion times. However, the scaling of the x-ray radiated energy is practically quadratic ($E_r \propto I^{1.9\pm0.24}$ to $E_r \propto I^{2.01\pm0.21}$). Our data were compared with the theoretical model of Stygar *et al.* [13] which appears to come closer to our results than the quadratic dependence model. Based on the experimental results of this work, the experimental results of Stygar *et al.* [13], the results of Nash *et al.* [18], and the heuristic model

of Stygar *et al.* [14], we derived two scaling relations for the implosion mechanisms and the peak radiated power scaling on the peak pinch current. More experimental work is needed in particular for evaluating the power and energy scaling of nested arrays, which are relevant to radiation pulse shaping for ICF applications of *z*-pinch x-ray sources [11].

The superior performance of the faster implosions may possibly be attributed to shorter ablation times and to lesser mass left behind at the initial array radius. It appears that 80-ns pinches may be more optimized for the *Z*-pinch driver. This data set provides constraints for large scale simulations with modern HEDP codes as well as for analytical work to understand how the peak x-ray radiated power and total energy from the wire-array *z* pinches relate to the driver peak current.

ACKNOWLEDGMENTS

The authors are deeply indebted to our colleagues at Sandia National Laboratories, Ktech Corporation, and Team Specialty Products. We also wish especially to thank the Z operation department headed by Guy L. Donovan, the supporting technologies department headed by Johann F. Seamen, the load design group headed by Dustin Heinz Romero, the diagnostics team headed by Don O. Jobe, and the wire array laboratory headed by Dolores Graham for their superb work and great dedication. The authors are grateful for helpful discussions with Dr. Sergey Lebedev and Dr. Simon Bland of the Imperial College. Sandia is a multiprogram laboratory operated by Sandia Corporation, a Lockheed Martin Company, for the U.S. Department of Energy under Contract No. DE-AC04-94-AL85000.

[1] T. W. L. Sanford, R. E. Olson, R. L. Bowers, G. A. Chandler, M. S. Derzon, D. E. Hebron, R. J. Leeper, R. C. Mock, T. J. Nash, D. L. Peterson, L. E. Ruggles, W. W. Simpson, K. W. Struve, and R. A. Vesey, Phys. Rev. Lett. **83**, 5511 (1999).

[2] C. Deeney, T. J. Nash, R. B. Spielman, J. F. Seamen, G. C. Chandler, K. W. Struve, J. L. Porter, W. A. Stygar, J. S. McGurn, D. O. Jobe, T. L. Gilliland, J. A. Torres, M. F. Vargas, L. E. Ruggles, S. Breeze, R. C. Mock, M. R. Douglas, D. L. Fehl, D. H. McDaniel, M. K. Matzen, D. L. Peterson, W. Matuska, N. F. Roderick, and J. J. MacFarlane, Phys. Rev. E **56**, 5945 (1997).

[3] M. K. Matzen, M. A. Sweeney, R. G. Adams, J. R. Asay, J. E. Bailey, G. R. Bennett, D. E. Bliss, D. D. Bloomquist, T. A. Brunner, R. B. Campbell, G. A. Chandler, C. A. Coverdale, M. E. Cuneo, J.-P. Davis, C. Deeney, M. P. Desjarlais, G. L. Donovan, C. J. Garasi, T. A. Haill, C. A. Hall, D. L. Hanson, M. J. Hurst, B. Jones, M. D. Knudson, R. J. Leeper, R. W. Lemke, M. G. Mazarakis, D. H. McDaniel, T. A. Mehlhorn, T. J. Nash, C. L. Olson, J. L. Porter, P. K. Rambo, S. E. Rosenthal, G. A. Rochau, L. E. Ruggles, C. L. Ruiz, T. W. Sanford, J. F. Seamen, D. B. Sinars, S. A. Slutz, I. C. Smith, K. W. Struve, W. A. Stygar, R. A. Vesey, E. A. Weinbrecht, D. F. Wenger, and E. P. Yu, Phys. Plasmas **12**, 055503 (2005).

[4] M. E. Cuneo, R. A. Vesey, G. R. Bennett, D. B. Sinars, W. A. Stygar, E. M. Waisman, J. L. Porter, P. K. Rambo, I. C. Smith, S. V. Lebedev, J. P. Chittenden, D. E. Bliss, T. J. Nash, G. A. Chandler, B. B. Afeyan, E. P. Yu, R. B. Campbell, R. G. Adams, D. L. Hanson, T. A. Mehlhorn, and M. K. Matzen, Plasma Phys. Controlled Fusion **48**, R1 (2006).

[5] R. A. Vesey, M. C. Hermann, R. W. Lemke, M. P. Desjarlais, M. E. Cuneo, W. A. Stygar, G. R. Bennett, R. B. Camppbell, P. J. Christenson, T. A. Mehlhorn, J. L. Porter, and S. A. Slutz, Phys. Plasmas **14**, 056302 (2007).

[6] J. H. Hammer, M. Tabak, S. C. Wilks, J. D. Lindl, D. S. Bailey, P. W. Rambo, A. Toor, G. B. Zimmerman, and J. L. Porter, Jr., Phys. Plasmas **6**, 2129 (1999).

[7] S. V. Lebedev, S. V. Lebedev, F. N. Beg, S. N. Bland, J. P. Chittenden, A. E. Dangor, M. G. Haines, K. H. Kwek, S. A. Pikuz, and T. A. Shelkovenko, Phys. Plasmas **8**, 3734 (2001).

[8] M. E. Cuneo, E. M. Waisman, S. V. Lebedev, J. P. Chittenden, W. A. Stygar, G. A. Chandler, R. A. Vesey, E. P. Yu, T. J. Nash, D. E. Bliss, G. S. Sarkisov, T. C. Wagoner, G. R. Bennett, D. B. Sinars, J. L. Porter, W. W. Simpson, L. E. Ruggles, D. F. Wenger, C. J. Garasi, B. V. Oliver, R. A. Arasgon, W. E. Fowler, M. C. Hettrick, G. C. Idzorek, D. Johnson, K. Keller, S. E. Lazier, J. S. McGurn, T. A. Mehlhorn, T. Moore, D. S. Nielsen, J. Pyle, S. Speas, K. W. Struve, and J. A. Torres, Phys. Rev. E **71**, 046406 (2005).

[9] D. B. Sinars, M. E. Cuneo, E. P. Yu, D. E. Bliss, T. J. Nash, J. L. Porter, C. Deeney, M. G. Mazarakis, G. S. Sarkisov, and D. F. Wenger, Phys. Rev. Lett. **93**, 145002 (2004).

[10] D. B. Sinars, M. E. Cuneo, E. P. Yu, S. V. Lebedev, K. R. Cochrane, B. Jones, J. J. McFarlane, T. A. Mehlhorn, J. L. Porter, and D. F. Wenger, Phys. Plasmas **13**, 042704 (2006).

[11] M. E. Cuneo, D. B. Sinars, E. M. Waisman, D. E. Bliss, W. A. Stygar, R. A. Vesey, R. W. Lemke, I. C. Smith, P. K. Rambo, J. L. Porter, G. A. Chandler, T. J. Nash, M. G. Mazarakis, R. G. Adams, J. P. Chittenton, S. Lebeolev, E. P. Yu, K. W. Struve, and T. A. Mehlhorn, Phys. Plasmas **13**, 056318 (2006).

[12] J. P. Chittenden, S. V. Lebedev, C. A. Jennings, S. N. Bland, and A. Ciardi, Plasma Phys. Controlled Fusion **46**, B457 (2004).

[13] W. A. Stygar, H. C. Ives, D. L. Fehl, M. E. Cuneo, M. G. Mazarakis, J. E. Bailey, G. R. Bennett, D. E. Bliss, G. A. Chandler, R. J. Leeper, M. K. Matzen, D. H. McDaniel, J. S. McGurn, J. L. McKenney, L. P. Mix, D. J. Muron, J. L. Porter, J. J. Ramirez, L. E. Ruggles, J. F. Seamen, W. W. Simpson, C. S. Speas, R. B. Spielman, K. W. Struve, J. A. Torres, R. A. Vesey, T. C. Wagoner, T. L. Gilliland, M. L. Horry, D. O. Jobe, S. E. Lazier, J. A. Mills, T. D. Mulville, J. H. Pyle, T. M. Romero, J. J. Seamen, and R. M. Smelser, Phys. Rev. E **69**, 046403 (2004).

[14] W. A. Stygar, M. E. Cuneo, R. A. Vesey, H. C. Ives, M. G. Mazarakis, G. A. Chandler, D. L. Fehl, R. J. Leeper, M. K. Matzen, D. H. McDaniel, J. S. McGurn, J. L. McKenney, D. J. Muron, C. L. Olson, J. L. Porter, J. J. Ramirez, J. F. Seamen, C. S. Speas, R. B. Spielman, K. W. Struve, J. A. Torres, and E. M. Waisman, Phys. Rev. E **72**, 026404 (2005).

[15] M. K. Matzen, Phys. Plasmas **4**, 1519 (1997).
[16] M. A. Liberman, J. S. De Groot, A. Toor, and R. B. Spielman, *Physics of High-Density Z-Pinch Plasmas* (Springer, New York, 1999).
[17] R. B. Spielman and J. S. De Groot, Laser Part. Beams **19**, 509 (2001).
[18] T. Nash *et al.*, Phys. Plasmas **11**, 5156 (2004).
[19] D. B. Sinars, R. W. Lembe, M. E. Cuneo, S. V. Lebedev, E. M. Waisman, W. A. Stygar, B. Jones, M C. Jones, E. P. Yu, J. L. Porter, and D. F. Wenger, Phys. Rev. Lett. **100**, 145002 (2008).
[20] M. E. Cuneo (private communication).
[21] R. B. Spielman *et al.*, in *Proceedings of the 11th IEEE International Pulsed Power Conference*, edited by G. Cooperstein and I. Vitkovitsky (IEEE, Baltimore, 1997), p. 709.
[22] P. A. Corcoran *et al.*, in *Proceedings of the 11th IEEE International Pulsed Power Conference*, edited by G. Cooperstein and I. Vitkovitsky (IEEE, Baltimore, 1997), p. 466.
[23] R. J. Garcia *et al.*, in *Proceedings of the 11th IEEE International Pulsed Power Conference*, edited by G. Cooperstein and I. Vitkovitsky (IEEE, Baltimore, 1997), p. 1614.
[24] H. C. Ives *et al.*, in *Proceedings of the 11th IEEE International Pulsed Power Conference*, edited by G. Cooperstein and I. Vitkovitsky (IEEE, Baltimore, 1997), p. 1602.
[25] M. A. Mostrom *et al.*, in *Proceedings of the 11th IEEE International Pulsed Power Conference*, edited by G. Cooperstein and I. Vitkovitsky (IEEE, Baltimore, 1997), p. 460.
[26] R. W. Shoup *et al.*, in *Proceedings of the 11th IEEE International Pulsed Power Conference*, edited by G. Cooperstein and I. Vitkovitsky (IEEE, Baltimore, 1997), p. 1608.
[27] I. D. Smith *et al.*, in *Proceedings of the 11th IEEE International Pulsed Power Conference*, edited by G. Cooperstein and I. Vitkovitsky (IEEE, Baltimore, 1997), p. 168.
[28] K. W. Struve *et al.*, in *Proceedings of the 11th IEEE International Pulsed Power Conference*, edited by G. Cooperstein and I. Vitkovitsky (IEEE, Baltimore, 1997), p. 162.
[29] W. A. Stygar *et al.*, in *Proceedings of the 11th IEEE International Pulsed Power Conference*, edited by G. Cooperstein and I. Vitkovitsky (IEEE, Baltimore, 1997), p. 591.
[30] M. L. Kiefer, K. L. Fugelso, K. W. Struve, and M. M. Widner, "SCREAMER, A Pulsed Power Design Tool," User's Guide for Version 2.0, Sandia National Laboratory, 1995.
[31] M. G. Mazarakis, C. E. Deeney, M. R. Douglas, W. A. Stygar, D. B. Sinars, M. E. Cuneo, J. Chittenden, G. A. Chandler, T. J. Nash, K. W. Struve, and D. H. McDaniel, Plasma Devices Oper. **13**, 157 (2005).
[32] G. A. Chandler, C. Deeney, M. Cuneo, D. L. Fehl, J. S. McGurn, R. B. Spielman, J. A. Torres, J. L. McKenney, J. Mills, and K. W. Struve, Rev. Sci. Instrum. **70**, 561 (1999).
[33] R. B. Spielman, C. Deeney, D. L. Fehl, D. L. Hanson, N. R. Keltner, J. S. McGurn, and J. L. McKenney, Rev. Sci. Instrum. **70**, 651 (1999).
[34] D. L. Fehl, D. J. Muron, R. J. Leeper, G. A. Chandler, C. Deeney, W. A. Stygar, and R. B. Spielman, Rev. Sci. Instrum. **70**, 270 (1999).
[35] L. E. Ruggles, R. B. Spielman, J. L. Porter, Jr., and S. P. Breeze, Rev. Sci. Instrum. **66**, 712 (1995).
[36] L. E. Ruggles, J. L. Porter, W. W. Simpson, and M. F. Vargas, Rev. Sci. Instrum. **70**, 646 (1999).
[37] B. Jones, C. A. Coverdale, and M. G. Mazarakis, IEEE Trans. Plasma Sci. **36** (), 5822 (20070
[38] D. L. Fehl, W. A. Stygar, G. A. Chandler, M. E. Cuneo, and C. L. Ruiz, Rev. Sci. Instrum. **76**, 103504 (2005).
[39] W. A. Stygar *et al.*, *Proceedings of the 11th IEEE International Pulsed Power Conference*, edited by G. Cooperstein and I. Vitkovitsky (IEEE, Baltimore, 1997), p. 1258.
[40] T. C. Wagoner, W, A. Stygar, H. C. Ives, T. L. Gilliland, R. B. Spielman, M. F. Johnson, P. G. Reynolds, J. K. Moore, R. L. Mourning, D. L. Fehl, K. E. Androlewicz, J. E. Bailey, R. S. Broyles, T. A. Dinwoodie, G. L. Donovan, M. E. Dudley, K. D. Hahn, A. A. Kim, J. R. Lee, R. J. Leeper, G. T. Leifeste, J. A. Melville, J. A. Mills, L. P. Mix, W. B. S. Moore, B. P. Peyton, J. L. Porter, G. A. Rochau, G. E. Rochau, M. E. Savage, J. F. Seamen, J. D. Serrano, A. W. Sharpe, R. W. Shoup, J. S. Slopek, C. S. Speas, K. W. Struve, D. M. Van De Valde, and R. M. Woodring, Phys. Rev. ST Accel. Beams **11**, 100401 (2008).
[41] T. W. L. Sanford, R. C. Mock, R. B. Spielman, D. L. Peterson, D. Mosher, and N. F. Roderick, Phys. Plasmas **5**, 3737 (1998).
[42] D. D. Ryutov, M. S. Derzon, and M. K. Matzen, Rev. Mod. Phys. **72**, 167 (2000).
[43] J. R. Taylor, *An Introduction to Error Analysis* (University Science Books, Sausalito, CA, 1997).
[44] E. M. Waisman, M. E. Cuneo, W. A. Stygar, R. W. Lemke, K. W. Struve, and T. C. Wagoner, Phys. Plasmas **11**, 2009 (2004).
[45] D. L. Peterson, R. L. Bowers, K. D. McLenithan, C. Deeney, G. A. Chandler, R. B. Spielman, M. K. Matzen, and N. F. Roderick, Phys. Plasmas **5**, 3302 (1998).
[46] S. V. Lebedev, D. A. Hammer, M. E. Cuneo, and D. B. Sinars, in Dense Z-Pinches; 6th International Conference on Dense Z-Pinches, edited by J. Chittenden (American Institute of Physics, New York, 2006), p. 73.